Mathematical Modelling Of A Plate Type Heat Exchanger For A 0.1 MWe OTEC Plant

Vijayakrishna Rapaka E*, Michael Bakkiyanathan D**
*Former Assistant Professor, Department of Mechanical Engineering, Pondicherry Engineering College, Puducherry India
**Former PG Student, Department of Mechanical Engineering, Pondicherry Engineering College, Puducherry India

Abstract

The search for renewable sources of energy resulted in the revival of a concept "Ocean Thermal Energy Conversion" which utilizes the difference in temperature between the warm tropical surface waters and the cold deep ocean water available at depths of about 1000 m operating in a Rankine cycle. The heat exchangers are the major components of the OTEC power plants and they play an important role in the economy of the OTEC power plants, hence a proper selection of materials, design criteria, working fluid and working conditions for the heat exchangers are necessary for an energy efficient and techno-economically feasible OTEC power plant. The following parameters: pipe length, pipe diameter, seawater depth and the flow rate of seawater were considered. The theoretical investigations revealed that a maximum output of the net work exists at a certain flow rate of cooling seawater. In this report, the design of heat exchanger for a 0.1 MWe OTEC power plant is carried out and the performance of the heat exchanger for varying depths, for varying velocities of the intake fluid, for varying mass fraction of the working fluid, for varying length of the plates is simulated using Engineering Equations Solver. In addition, the variation in the Reynolds number, Nusselt number, Pressure drop and Overall heat transfer coefficient for varied process conditions are estimated and presented in graphical form.

1. Introduction

The ocean thermal energy concept was proposed as early as 1881 by the French physicist Jacques d' Arsonoval. This is an indirect form of collection and storage of solar energy. The surface of the water acts as the huge collector for solar heat thereby acting as an infinite heat storage reservoir. The heat thus collected in the oceans can be converted into electricity by utilizing the temperature difference between the warm surface water of the tropical oceans and the colder waters in the depths which is about 20 – 25 K using a rankine cycle. The above concept of utilization of this temperature difference in a heat engine to generate power is called ocean thermal energy conversion (OTEC). The amount of energy available for the ocean thermal power generation is enormous, and is replenished continuously. The surface temperature depends on the latitude and season. Based on the latitude and season, it is evident that the surface water temperatures are maximum in the tropical, sub-tropical, and equatorial waters i.e., between the tropics, making these waters the most suitable for OTEC systems. There are two different methods for harnessing ocean thermal differences. One is the Open cycle, also known as the Claude cycle, and other is the closed cycle system, also known as the Anderson cycle.

1.1. Open cycle OTEC system

The Claude cycle or open cycle utilizes the vapor pressure of sea water itself as the working medium and has been demonstrated to be practicable. Open cycle refers to the utilization of sea water by flash evaporating the working fluid under partial vacuum conditions. The low pressure steam thus obtained is passed through a turbine for extracting energy and the spent vapor is cooled in a condenser. This cycle drives the name open form the fact that the condensate is never returned to the evaporator instead the condensate is utilized as desalinated water using a surface condenser or a spray (direct-contact) condenser.

Very large ocean water and volume flow rates are used in the open OTEC systems and the turbine operating at a very low pressure receive requires specific volumes more than 2000 times in comparison to the specific volume requirement in a modern fossil fuel power plant. Due to the high specific volumes extremely large turbines must be used. In addition, degasifiers are essential to remove the gases dissolved in the sea water.

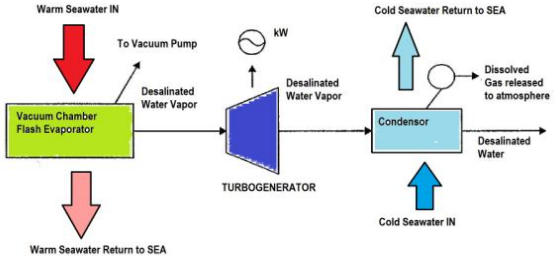

Figure 1. Open cycle OTEC system

1.2. Closed cycle OTEC system

The closed cycle was first proposed by Barjot in 1926, but the most recent design was by Anderson in 1960. In this cycle, propane or ammonia can be used as a working fluid. The temperature difference between warm surface and cold water from the deep is 20 °C. The cold water is pumped from a depth of 600 m. The working fluid is vaporized in the boiler (evaporator) at 10 bar and exhausted in the condenser at 5 bar. The high pressure vapor leaving the evaporator enters an expansion turbine thereby producing useful energy. The useful mechanical energy from the turbine is converted toe electrical energy using and an electric generator. The low pressure exhaust from the turbine is cooled and converted back into liquid in the condenser. The cooling is achieved by passing cold, deep ocean water, from a depth of 700 to 900m or more, through a heat exchanger. The liquid working fluid is then pumped back as high pressure liquid to the evaporator, thus closing the cycle.

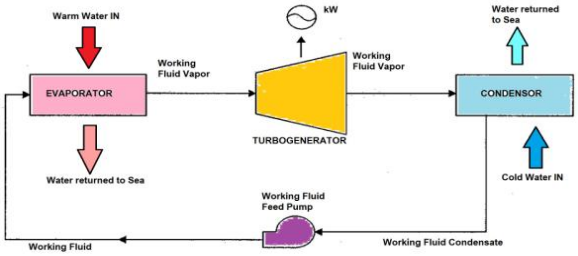

Figure 2. Closed cycle OTEC system

2. Literature Survey

Mitseuteru, K., and Ikegami,Y., [[8]] have carried out the performance evaluation of the overall heat transfer coefficient and boiling heat transfer coefficients of a plate type evaporator using ammonia/ water mixtures. Uehara, H., and Ikegami, Y., [[16]] have carried out study on the Optimization of an OTEC power plant with plate type heat exchangers and concluded that the plate heat exchangers produce better heat transfer rates when compared to the shell and tube heat exchangers. Uehara, H., et al [[17]] carried out studies on the performance of an OTEC power plant with ammonia and water as working fluid and concluded that the performance of the plant increases when compared to other combinations with fewer factors of safety. Tsutomo Nakaoa and Uehara [[15]] have carried out experiments with Shell and Plate Heat exchangers (evaporator) and with Freon12 and have found that the Overall heat transfer coefficient increases. Paras, S.V. et al [[12]] have studied the various diameters of the tubes used for the heat transfer in the plate type heat exchanger and the flooding effect that takes place in the small diameter tubes in the case of vertical tubes and the effect of the inclination angle in the plate type heat exchangers. Paras, S.V. et al [[11]] have studied the effect of grooves in the plate type exchanger. The channel used for the simulation is formed by only one corrugated plate, and two side-grooves, while the other plate is flat. The various Reynolds numbers used have been ranging form 250-1150. A standard k-ε model was used for the calculations and, in addition to isothermal flow, heat transfer simulations were carried out for the case of hot air. Focke et al [[3]] have studied the performance of the plate type heat exchanger with various angles of inclination and also the effect of flow and heat transfer properties for a given hydraulic diameter of the heat exchanger. Hesselgraves, J. E., [[6]] has studied and formulated some design criteria and some operating conditions for the compact type heat exchangers and also the performance characteristics of these heat exchangers. Wongwises, S., [[18]] has studied the effect of the inclination angle in the straight pipes and has compared the results with that of the vertical pipes and upper end conditions on the countercurrent flow limitation in straight circular pipes. Mitsumeri et al [[14]] have carried out performance studies of a plate type heat exchanger by comparing it with a double-fluted tube type exchanger. They have fond that the plate type heat exchanger offers more performance than the tube type heat exchanger. Blomerius, H and Mitra, N.K., [[1]] have made numerical investigation on the heat transfer and pressure drop in wary ducts and have found that the pressure drop increases varies with the duct diameter and the convective heat transfer also increases. Focke, W and Knibbe, P.G., [[2]] have carried out CFD analyses on the flow of the fluid inside the parallel-plates ducts with corrugated wall and have found that the inclination angle or the chevron angle plays an important role in the efficient performance of the parallel plate ducts. Further the efficiency of the ducts is increased by the use of corrugated walls as more surface heat transfer is obtained. Sriyutha Murthy, P et al [[10]] have suggested Bio-film control for the plate heat exchangers using surface

seawater from the for a OTEC power plant for the efficient reduction of the fouling in the heat exchanger which is the major disadvantage has the plate type heat exchanger must be covered with thin films for the plates to be held in a tight manner. Allen, H.G., and Karayiannis, T.G., [[9]] have considered the case for using electro hydrodynamic (EHD) enhancement of heat transfer in thermodynamic renewable energy applications where temperature levels are relatively low. They also established the basis on which nucleate boiling heat transfer is enhanced by EHD forces at surfaces designed to improve condensation, giving experimental results for a six-tube, shell/tube heat exchanger for boiling R12. Heavner, R.L., et al [[4]] have studied the performance characteristics of a plate type heat exchanger which is used for industrial purpose and the effect of the chevron angle on the performance characteristics of the heat exchanger. Heggs, P.J., et al [[5]] has investigated the effect of the local transfer coefficients which plays a major role in the efficient and techno-economically design of a heat exchanger. It is found that the local heat transfer increases. Kays, W.M. and London, A.L., [[7]] have made extensive research on the compact type heat exchangers. They have studied the effect of fins in increasing the effectiveness of the heat exchangers and have obtained various results on the effect of fins on the design parameters of a compact type heat exchanger. Shah, R.K. and Wanniarachi, A.S., [[13]] have proposed the design procedures for a plate type heat exchanger used for industrial purposes.

3. Heat Exchangers

Heat exchangers are devices used for transfer of heat from one flowing fluid to another through a solid barrier separating these fluids. There are various types of heat exchangers used for the purpose of heat exchange between two fluids. Heat exchangers are basically classified according to flow arrangement and type of construction. The following are the types of heat exchangers most commonly used in the industrial applications.

3.1. Double pipe heat exchanger

The simplest heat exchanger is one for which the hot and cold fluids move in same or opposite direction in a concentric tube which is otherwise called as the double pipe heat exchanger. The two types of flow arrangement in the double pipe heat exchanger is the Parallel and Counterflow arrangement. In the parallel flow arrangement the hot and cold fluids enter at the same end, flow in the same direction, and both the fluids exits at the opposite end. In the counterflow arrangement the fluids enter at the opposite ends, flow in the reverse directions relative to each other direction and leave at opposite ends.

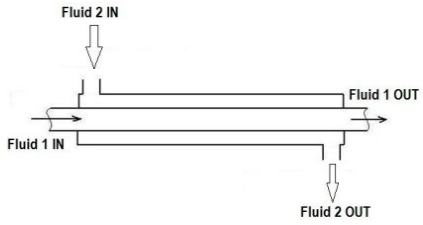

Figure 3. Double pipe heat exchanger

3.2. Shell and Tube heat exchanger

Another common configuration of heat exchanger is the Shell and Tube type heat exchangers. This type of heat exchanger is widely used in the chemical process industries. In this type one fluid flows on the inside of the tubes while the other fluid is forced through the shell and over the surface of the tubes. To ensure that the shell side fluid will flow across the tubes uniformly in order to induce higher heat transfer, baffles are placed in the shell at pre-determined locations. Depending on the head arrangement at the ends of the heat exchanger, one or more tube passes can be provided.

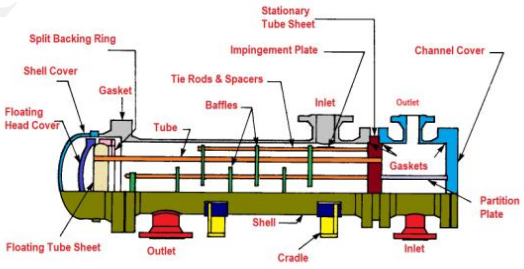

Figure 4. Shell and tube heat exchanger

In this exchanger the gas flowing across the tubes is mixed stream, while the fluid in the tubes is unmixed. The gas shows a mixed flow behavior as it is allowed to move about freely in the exchanger as it exchanges heat. The unmixed fluid is confined in the separate tubular channels in the heat exchanger thereby preventing the fluid to get mixed during the heat transfer process.

3.3. Plate Type Heat exchangers:

The plates which are the main components of the plate heat exchanger are attached together in a large frame with rubber gaskets that are placed between each plate. There are four flow ports on each plate. The gasket blocks one top and one bottom port so that the fluid flows by the remaining two open ports. This will be reversed for the next plate countercurrentwise. This arrangement improves considerably the heat transfer between

the two fluids and ensures non mixing of the flowing fluids.

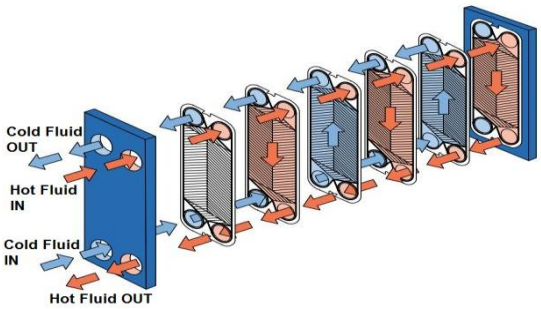

Figure 5. Plate type heat exchanger

Advantages of plate heat exchangers over shell and tube heat exchangers

- High overall heat transfer coefficient
- Low cost
- Lower space requirement
- Easy maintenance
- Less weight
- Lower heat loss

However, they also have a few disadvantages such as being not suitable for temperatures higher than 200°C and pressures higher than 20 bar. Additionally, the fluids must have a maximum viscosity of 10 Pa. s. Since the temperature handled in warm water is around 25 – 30 °C and pressure around 10 bar, the plate type heat exchanger can be used for OTEC power plants.

4. Design of plate type heat exchanger)

Plate length	0.400 *m*
Plate width	0.123 *m*
Mean spacing between plates, b	0.024 *m*
Corrugation angle / Chevron Angle	60°
Port-to-port length	0.352 *m*
Plate width inside gasket, w	0.100 *m*
No. of Plates	100
Outer Diameter of the tube	$13*10^{-3}$ *m*
Inner Diameter of the tube	$7*10^{-2}$ *m*

4.1. Hot fluid side (T_h = 288 K)

Average Temperatures for hot fluid side

T_{avg} = 288 *K*

Table 1. Fluid properties for the average temperature (288 *K*)

Parameters	Hot Fluid	Units
Density	630.7000	kg/m^3
Specific heat	4.648	kJ/kgK
Thermal conductivity	0.5254	W/mK
Viscosity	0.1777	kg/ms
Prandtl number	1.5720	Dimensionless number
Velocity of the fluid	2.0000	m/s^2

Mass flow rate

$$m = \rho \times a \times u$$
$$m = 630.7 \times 1.327 \times 10^{-4} \times 2$$
$$m = 0.1674 \ kg/s$$
$$q = m \times C_p \times \Delta T$$
$$q = 0.16742851 \times 4.648 \times 288$$
$$q = 224.123 \ kJ/kgK$$

Reynolds number

$$\mathrm{Re} = \frac{u \times \rho \times D_e}{\mu}$$
$$D_e = 2 \times \text{Width of the corrugated plate}$$
$$D_e = 2 \times 0.01$$
$$D_e = 0.02 \ m$$
$$\mathrm{Re} = \frac{2 \times 630.7 \times (2 \times 0.01)}{0.1777}$$
$$\mathrm{Re} = 142$$

Nusselt Number

$$Nu = 0.28 \times (\mathrm{Re})^{0.8} \times (\mathrm{Pr})^{0.4}$$
$$Nu = 0.28 \times (142)^{0.8} \times (1.572)^{0.4}$$
$$Nu = 17.68$$

Heat transfer coefficient

$$Nu = \frac{h \times D_e}{k}$$
$$h = \frac{Nu \times k}{D_e}$$
$$h = \frac{17.68 \times 0.5254}{(2 \times 0.01)}$$
$$h = 464.47 \ W/mK$$

Number of transfer units

$$NTU = \frac{\Delta T}{LMTD}$$
$$LMTD = \frac{\Delta T}{NTU}$$
$$LMTD = \frac{288}{2}$$
$$LMTD = 144^\circ C$$

Design overall heat transfer coefficient

$$U = \frac{Q}{LMTD \times A}$$

$$U = \frac{0.1 \times 10^{6}}{144 \times \left(\pi \times 17 \times 10^{-3}\right) \times 0.400}$$

$$U = 43880\ W/m^2K$$

$$U = 43.88\ KW/m^2K$$

Mass velocity

$$G_m = \frac{m}{N_p \times w \times D_e}$$

$$G_m = \frac{0.1674}{50 \times 0.123 \times (2 \times 0.01)}$$

$$G_m = 978.3\ kg/m^2s$$

Pressure drop

$$\Delta P = \frac{2 \times f \times G_m \times L}{g \times \rho \times D_e}$$

$$N_p = \frac{(N-1)}{2}$$

$$N_p = \frac{(100-1)}{2}$$

$$N_p = 50$$

$$f = \left(\frac{978.3 \times (2 \times 0.01)}{0.1777}\right)^{-0.3}$$

$$f = 0.6101$$

$$\Delta P = \frac{2 \times 0.1601 \times 978.3 \times 0.400}{9.81 \times 630.7 \times (2 \times 0.01)}$$

$$\Delta P = 3775\ Pa$$

$$\Delta P = 3.775\ kPa$$

4.2. Cold fluid side (T_c = 279 K)

Average Temperatures for hot fluid side

T_{avg} = 279 *K*

Table 2. Fluid properties for the average temperature (279 *K*)

Parameters	Cold Fluid	Units
Density	999.4000	kg/m^3
Specific heat	4.1840	kJ/kgK
Thermal conductivity	0.5759	W/mK
Viscosity	1.1580	kg/ms
Prandtl number	8.4080	Dimensionless
		number
Velocity of the fluid	2.0000	m/s^2

Mass flow rate

$$m = \rho \times a \times u$$

$$m = 1000 \times 1.327 \times 10^{-4} \times 2$$

$$m = 0.2654\ kg/s$$

$$q = m \times C_p \times \Delta T$$

$$q = 0.2654 \times 4.184 \times 279$$

$$q = 309.886\ kJ/kgK$$

Reynolds number

$$\mathrm{Re} = \frac{u \times \rho \times D_e}{\mu}$$

$$D_e = 2 \times \text{Width of the corrugated plate}$$

$$D_e = 2 \times 0.01$$

$$D_e = 0.02\ m$$

$$\mathrm{Re} = \frac{2 \times 9994.4 \times (2 \times 0.01)}{1.158}$$

$$\mathrm{Re} = 34.52$$

Nusselt number

$$Nu = 0.28 \times (\mathrm{Re})^{0.8} \times (\mathrm{Pr})^{0.4}$$

$$Nu = 0.28 \times (34.52)^{0.8} \times (8.408)^{0.4}$$

$$Nu = 11.60$$

Heat transfer coefficient

$$Nu = \frac{h \times D_e}{k}$$

$$h = \frac{Nu \times k}{D_e}$$

$$h = \frac{11.60 \times 0.5759}{(2 \times 0.01)}$$

$$h = 321.3\ W/mK$$

Number of transfer units

$$NTU = \frac{\Delta T}{LMTD}$$

$$LMTD = \frac{\Delta T}{NTU}$$

$$LMTD = \frac{279}{2}$$

$$LMTD = 139.5^{\circ}C$$

Design overall heat transfer coefficient

$$U = \frac{Q}{LMTD \times A}$$

$$U = \frac{0.1 \times 10^6}{139.5 \times \left(\pi \times 17 \times 10^{-3}\right) \times 0.400}$$

$$U = 42510\ W/m^2K$$

$$U = 42.51\ KW/m^2K$$

Mass velocity

$$G_m = \frac{m}{N_p \times w \times D_e}$$

$$G_m = \frac{0.2654}{50 \times 0.123 \times (2 \times 0.01)}$$

$$G_m = 1550\ kg/m^2s$$

Pressure drop

$$\Delta P = \frac{2 \times f \times G_m \times L}{g \times \rho \times D_e}$$

$$N_p = \frac{(N-1)}{2}$$

$$N_p = \frac{(100-1)}{2}$$

$$N_p = 50$$

$$f = \left(\frac{999.4 \times (2 \times 0.01)}{1.158}\right)^{-0.3}$$

$$f = 0.6101$$

$$\Delta P = \frac{2 \times 0.2654 \times 1550 \times 0.400}{9.81 \times 999.4 \times (2 \times 0.01)}$$

$$\Delta P = 9140\ Pa$$

$$\Delta P = 9.140\ kPa$$

Geometric characteristics of the corrugated Plate type heat exchanger

Plate length	0.400 *m*
Plate width	0.123 *m*
Mean spacing between plates, *b*	0.024 *m*
Corrugation angle / Chevron Angle	60°
Port-to-port length	0.352 *m*
Plate width inside gasket, *w*	0.100 *m*
Mean flow cross-section channel area, A_f	$3.88*10^{-4}\ m^2$
Heat transfer area, *A*	$2.51*10^{-2}\ m^2$
No. of Plates	100
Outer Diameter of the tube	$13*10^{-3}\ m$
Inner Diameter of the tube	$7*10^{-2}\ m$
Equivalent diameter, D_e	$2*10^{-2}\ m$
No. of passes, N_p	50

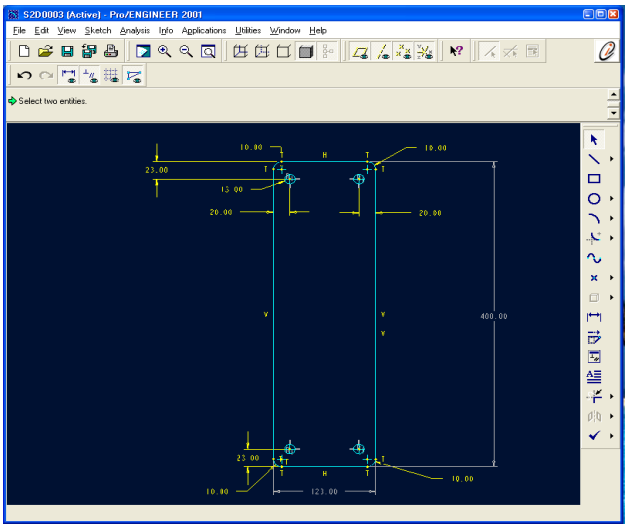

Figure 6. Design drawing of the plate type heat exchanger

5. Results and discussions

The various results obtained during the design of the plate type heat exchanger and the factors that influence the design of heat exchanger and their variations are plotted in a graph. The variation in the pressure drop, the variation in the overall heat transfer coefficient, the variation in the Reynolds number, the variation in the Nusselt number for both hot and cold fluid at different depths for different lengths are plotted. The factors affecting these parameters and the percentage increase or decrease for these parameters are discussed. Further the velocity which plays a major role in the heat exchangers has been also discussed. The variations that the velocity causes on the pressure drop for both hot and cold fluid for different lengths of the pipe at different depths have been plotted. The percentage increase of the pressure drop for the variation in the velocity intake at different depths for varying length of the plate is reported.

Figure 7 shows the effect of plate length on the pressure drop on the hot and the cold fluid side for various depths. The pressure drop decreases with the increase in the plate length. The pressure decreases because for the same velocity as the length increases the flow will be less turbulent thereby reducing the pressure drops. The percentage decrease in the pressure drop at depths 600 m, 700 m, 800 m, 900 m and 1000 m for the plate length from 400 - 500 is 62.5%, 60%, 66%, 67%, 50%. The percentage decrease in the pressure drop at depths 600 m, 700 m, 800 m, 900 m and 1000 m for the plate length from 500 - 600 is

28.25%, 75%, 60%, 86.65 %, 87.55%. The percentage decrease in the pressure drop at depths 600 m, 700 m, 800 m, 900 m and 1000 m for the plate length from 600 - 700 is 23%, 35%, 72%, 70%, 41.5%. The percentage decrease in the pressure drop at depths 600 m, 700 m, 800 m, 900 m and 1000 m for the plate length from 700 - 800 is 20%, 28%, 62%, 35.63%, 39.3%.

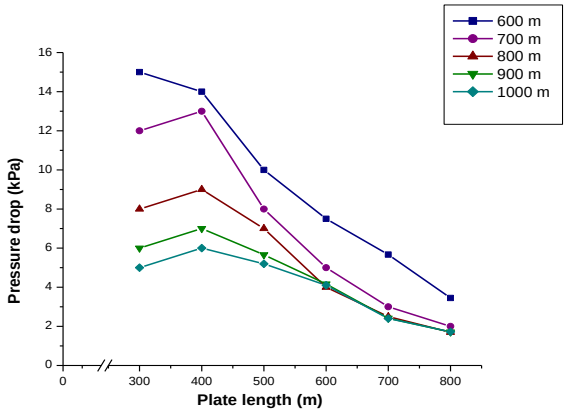

Figure 7. Comparison between the plate length and pressure drop at different depths

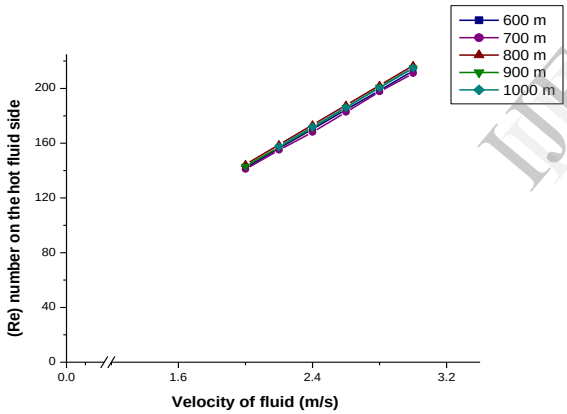

Figure 8. Comparison between the plate length and Reynolds number at different depths

Figure 8 shows the effect of the velocity of the fluid on the Reynolds number on the hot fluid side for a plate length of 0.4 m at various depths. Here the length is kept constant The Reynolds number increases with increases in the velocity because of the linear relationship. The Reynolds number should as small as possible in the corrugated plate type heat exchangers in order to avoid the flooding in the tubes along with the intake velocity of the fluid. The research work carried out by Mouza et al [[19]] for the plate length of 0.4 m and with a tube diameter of 7 mm shows that the Reynolds number is around 100-250 but the flooding in the use of small tube diameters is more when compared to the large tube diameters. The percentage increase of (Re) number at the depths 600 m, 700 m, 800 m, 900 m and 1000 m for a velocity of 2 - 2.2 is 9.09%, 8.2%, 7.6%, 7.2%, 7.05%. The percentage increase of (Re) number at the depths 600 m, 700 m, 800 m, 900 m and 1000 m for a velocity of 2.2 - 2.4 is 9.03%, 7.7%, 8.75%, 7.5%, 7.5%. The percentage increase of (Re) number at the depths 600 m, 700 m, 800 m, 900 m and 1000 m for a velocity of 2.4 - 2.6 is 9.03%, 8.3%, 7.6%, 7.2%, 7.16%. The percentage increase of (Re) number at the depths 600 m, 700 m, 800 m, 900 m and 1000 m for a velocity of 2.6 – 2.8 is 9.13%, 8.3%, 7.6%, 7.13%, 7.25%. The percentage increase of (Re) number at the depths 600 m, 700 m, 800 m, 900 m and 1000 m for a velocity of 2.8 – 3 is 9.13%, 8.3%, 7.6%, 7.13%, 7.25%.

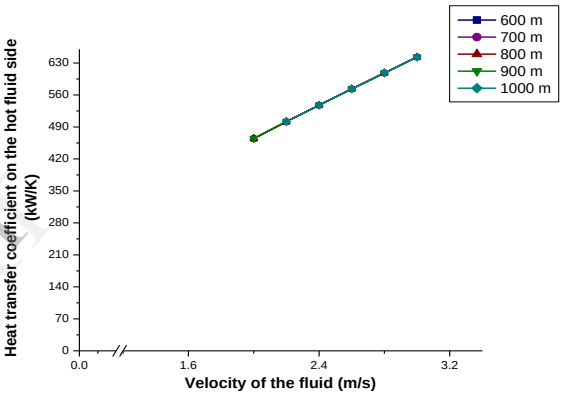

Figure 9 comparison between the plate length and heat transfer coefficient on the hot fluid side at various depths

Figure 9 shows the effect of the velocity of the fluid on the heat transfer coefficient on the hot fluid side for a plate length of 0.4 m at various depths. The heat transfer coefficient increases as the velocity of the fluid increases. The heat transfer coefficient increases because the nusselt number increases. The percentage increase of heat transfer coefficient at the depths 600 m, 700 m, 800 m, 900 m and 1000 m for a velocity of 2 - 2.2 is 7.3%, 6.7%, 6.14%, 5.75%, 5.55%. The percentage increase of heat transfer coefficient at the depths 600 m, 700 m, 800 m, 900 m and 1000 m for a velocity of 2.2 - 2.4 is 7.36%, 6.8%, 6.14%, 5.76%, 5.56% . The percentage increase of heat transfer coefficient at the depths 600 m, 700 m, 800 m, 900 m and 1000 m for a velocity of 2.4 - 2.6 is 7.38%, 6.21%, 6.7%, 6.13%, 5.8%. The percentage increase of (Re) number at the depths 600 m, 700 m, 800 m, 900 m and 1000 m for a velocity of 2.6 – 2.8 is 9.13%, 8.3%, 7.6%, 7.13%, 7.25%.The percentage increase of heat transfer coefficient at

the depths 600 m, 700 m, 800 m, 900 m and 1000 m for a velocity of 2.8-3 is 7.5%, 7%, 7.14%, 5.90%, 4.89%.

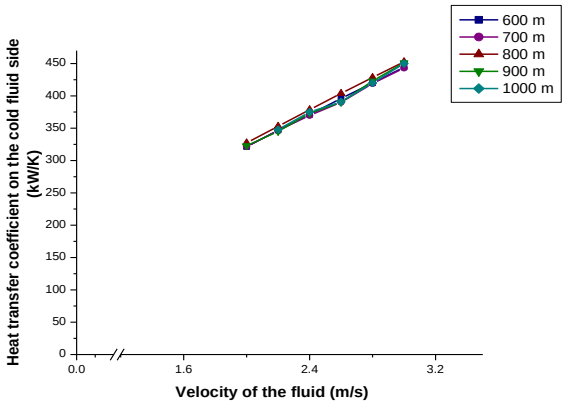

Figure 10. Comparison between the plate length and heat transfer coefficient on the cold fluid side at various depths

Figure 10 shows the effect of the velocity of the fluid on the heat transfer coefficient on the cold fluid side for a plate length of 0.4 m at various depths. The heat transfer coefficient increases as the velocity of the fluid increases. The heat transfer coefficient increases because the nusselt number increases. The percentage increase of heat transfer coefficient at the depths 600 m, 700 m, 800 m, 900 m and 1000 m for a velocity of 2 - 2.2 is 7.2%, 6.3%, 5.1%, 6.9%, 7.11%. The percentage increase of heat transfer coefficient at the depths 600 m, 700 m, 800 m, 900 m and 1000 m for a velocity of 2.2 - 2.4 is 7.21% , 6.4%, 5.25%, 6.95%, 6.0%. The percentage increase of heat transfer coefficient at the depths 600 m, 700 m, 800 m, 900 m and 1000 m for a velocity of 2.4 - 2.6 is 7.2%, 6.3%, 5.12%, 6.55%, 7%. The percentage increase of heat transfer coefficient at the depths 600 m, 700 m, 800 m, 900 m and 1000 m for a velocity of 2.6 - 2.8 is 7.23%, 6.7%, 5.13%, 6%, 6.66%. The percentage increase of heat transfer coefficient at the depths 600 m, 700 m, 800 m, 900 m and 1000 m for a velocity of 2.8 - 3 is 7.2%, 6.4%, 5.12%, 6.87%, 7%.

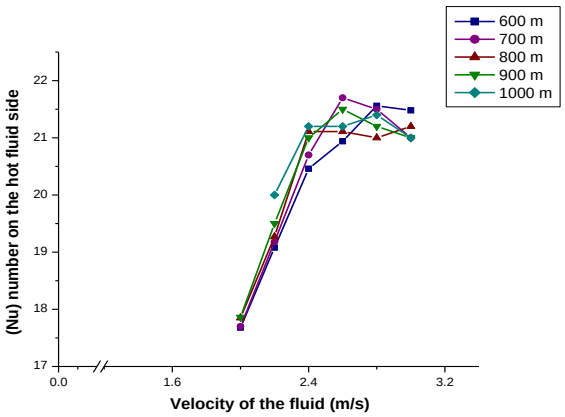

Figure 11. Comparison between the plate length and nusselt number on the hot fluid side at various depths

Figure 11 shows the effect of the velocity of the fluid on the Nusselt number on the hot fluid side for a Plate length of 0.4 m at various depths. The Nusselt number increases as the velocity of the fluid increases. Further the nusselt number is the dimensionless number which mainly depends on the effect of two other dimensionless numbers. As the Reynolds number and the Prandtl number increases the Nusselt number also increases. The percentage increase of Nusselt number at the depths 600m, 700m, 800m, 900m and 1000m for a velocity of 2 - 2.2 is 7.9%, 6.7%, 4.5%, 4.67%, 5%. The percentage increase of Nusselt number at the depths 600 m, 700 m, 800 m, 900 m and 1000 m for a velocity of 2.2 - 2.4 is 7.68%, 7.69%, 7.69%, 7%, 8% . The percentage increase of Nusselt number at the depths 600 m, 700 m, 800 m, 900 m and 1000 m for a velocity of 2.4 - 2.6 is 7.69%, 6.14%, 7.14%, 8.12%, 8%. The percentage increase of Nusselt number at the depths 600 m, 700 m, 800 m, 900 m and 1000 m for a velocity of 2.6 - 2.8 is 7.69%, 7.14%, 7.14%, 7.15%, 7.2%. The percentage increase of Nusselt number at the depths 600 m, 700 m, 800 m, 900 m and 1000 m for a velocity of 2.8 - 3 is 6.66%, 6.67%, 6.66%, 6.66%, 6.66%.

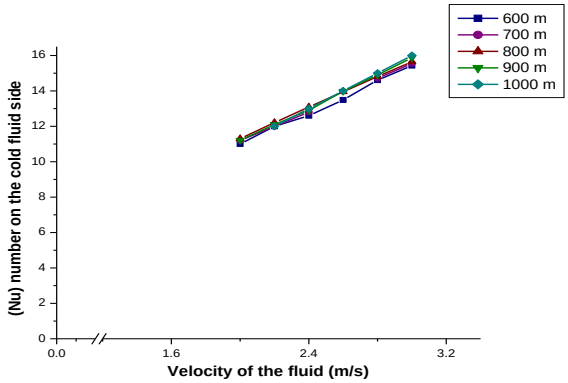

Figure 12. Comparison between the plate length and nusselt number on the cold fluid side at various depths

Figure 12 shows the effect of the velocity of the fluid on the Nusselt number on the cold fluid side for a Plate length of 0.4 m at various depths. The Nusselt number increases as the velocity of the fluid increases. Further the nusselt number is the dimensionless number which mainly depends on the effect of two other dimensionless numbers. As the Reynolds number and the Prandtl number increases the Nusselt number also increases. The percentage increase of Nusselt number at the depths 600 m, 700 m, 800 m, 900 m and 1000 m for a velocity of 2 - 2.2 is 8.32%, 4.56%, 4.76%, 6.59%, 5.3%. The percentage increase of Nusselt number at the depths 600 m, 700 m, 800 m, 900 m and 1000 m for a velocity of 2.2 - 2.4 is 6.66%, 6.25%, 5.18%, 8.22%, 8.5% . The percentage increase of Nusselt number at the depths 600 m, 700 m, 800 m, 900 m and 1000 m for a velocity of 2.4 - 2.6 is 7.4%, 6.72%, 5.2%, 5.18%, 8.22%. The percentage increase of Nusselt number at the depths 600 m, 700 m, 800 m, 900 m and 1000 m for a velocity of 2.6 - 2.8 is 6.66%, 6.67%, 6.66%, 6.66%, 6.5%. The percentage increase of Nusselt number at the depths 600 m, 700 m, 800 m, 900 m and 1000 m for a velocity of 2.8 - 3 is 6.58%, 7.69%, 7.14%, 6.22%, 6.25%.

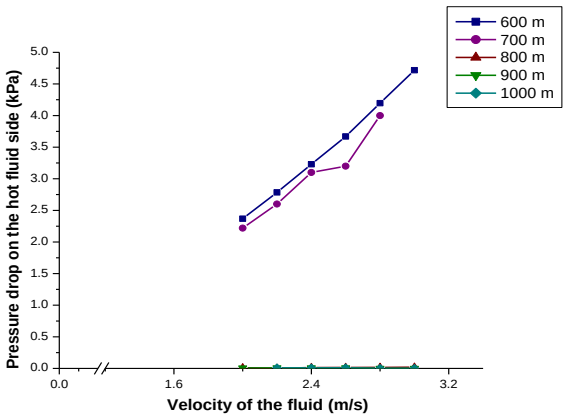

Figure 13. Comparison between the plate length and pressure drop on the hot fluid side at various depths

Figure 13 shows the effect of velocity of the fluid on the pressure drop on the hot fluid side for a plate length of 0.5 m at various depths. The pressure drop increases as the velocity of the fluid increases. The percentage increase of pressure drop at the depths 600 m, 700 m, 800 m, 900 m and 1000 m for a velocity of 2 - 2.2 is 8.32%, 6.76%, 6.59%, 7.3%, 7.12%. The percentage increase of pressure drop at the depths 600 m, 700 m, 800 m, 900 m and 1000 m for a velocity of 2.2 - 2.4 is 7.66%, 6.25%, 6.18%, 8.22%, 7.0%. The percentage increase of pressure drop at the depths 600 m, 700 m, 800 m, 900 m and 1000 m for a velocity of 2.4 - 2.6 is 7.4%, 6.72%, 5.18%, 8.22%, 8.12%. The percentage increase of pressure drop at the depths 600 m, 700 m, 800 m, 900 m and 1000 m for a velocity of 2.6 - 2.8 is 6.66%, 6.66%, 6.67%, 6.66%, 6.66%. The percentage increase of pressure drop at the depths 600 m, 700 m, 800 m, 900 m and 1000 m for a velocity of 2.8 - 3 is 7.58%, 7.69%, 7.14%, 7.22%, 6.25%.

Figure 14 shows the effect of velocity of the fluid on the pressure drop on the cold fluid side for a plate length of 0.5 m at various depths. The pressure drop increases as the velocity of the fluid increases. The percentage increase of pressure drop at the depths 600 m, 700 m, 800 m, 900 m and 1000 m for a velocity of 2 - 2.2 is 8.32%, 5.76%, 6.59%, 6.2%, 6.3%. The percentage increase of pressure drop at the depths 600 m, 700 m, 800 m, 900 m and 1000 m for a velocity of 2.2 - 2.4 is 6.66%, 6.25%, 6.18%, 8.22%, 6.78%. The percentage increase of pressure drop at the depths 600 m, 700 m, 800 m, 900 m and 1000 m for a velocity of 2.4 - 2.6 is 7.4%, 6.72%, 6.18%, 6.22%, 6.3%. The percentage increase of pressure drop at the depths 600 m, 700 m, 800 m, 900 m and 1000 m for a velocity of 2.6 - 2.8 is 6.66%, 7.76%, 7.66%, 7.66%, 7.22%. The percentage increase of

pressure drop at the depths 600 m, 700 m, 800 m, 900 m and 1000 m for a velocity of 2.8 - 3 is 7.58%, 7.69%, 7.14%, 7.22%, 6.25%.

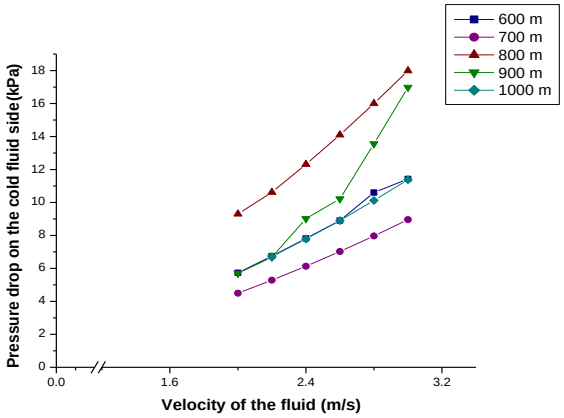

Figure 14. Comparison between the plate length and pressure drop on the cold fluid side at various depths

Figure 15 shows the effect of velocity of the fluid on the pressure drop on the hot fluid side for a plate length of 0.6 m at various depths. The pressure drop increases as the velocity of the fluid increases. The percentage increase of pressure drop at the depths 600m, 700m, 800m, 900m and 1000m for a velocity of 2 - 2.2 is 8.32%, 5.76%, 6.59%, 7.3%, 7.2%. The percentage increase of pressure drop at the depths 600 m, 700 m, 800 m, 900 m and 1000 m for a velocity of 2.2 - 2.4 is 7.66%, 7.25%, 7.18%, 8.22%, 7.2%. The percentage increase of pressure drop at the depths 600 m, 700 m, 800 m, 900 m and 1000 m for a velocity of 2.4 - 2.6 is 7.4%, 7.72%, 6.18%, 8.22%, 7.4%. The percentage increase of pressure drop at the depths 600 m, 700 m, 800 m, 900 m and 1000 m for a velocity of 2.6 - 2.8 is 7.66%, 7.67%, 6.66%, 8.66%, 9.12% . The percentage increase of pressure drop at the depths 600 m, 700 m, 800 m, 900 m and 1000 m for a velocity of 2.8 - 3 is 7.58%, 7.69%, 7.14%, 7.22%, 7.25%.

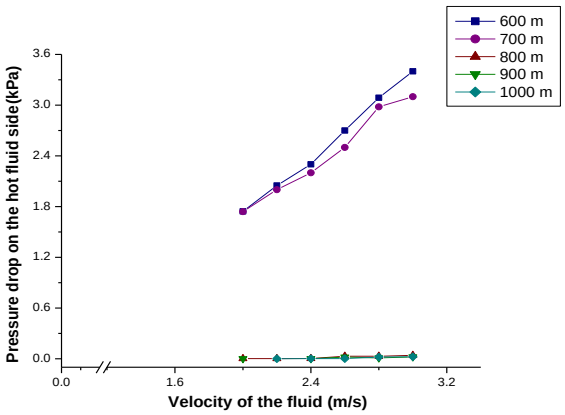

Figure 15. Comparison between the plate length pressure drop on the hot fluid side at various depths

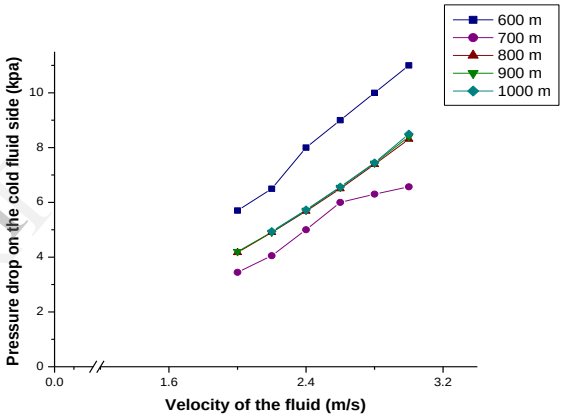

Figure 16. Comparison between the plate length pressure drop on the cold fluid side at various depths

Figure 16 shows the effect of velocity of the fluid on the pressure drop on the cold fluid side for a plate length of 0.6 m at various depths. The pressure drop increases as the velocity of the fluid increases. The percentage increase of pressure drop at the depths 600 m, 700 m, 800 m, 900 m and 1000 m for a velocity of 2 - 2.2 is 8.32%, 5.76%, 7.59%, 6.3%, 6.66%. The percentage increase of pressure drop at the depths 600 m, 700 m, 800 m, 900 m and 1000 m for a velocity of 2.2 - 2.4 is 6.66%, 7.25%, 6.18%, 8.22%, 6.56%. The percentage increase of pressure drop at the depths 600 m, 700 m, 800 m, 900 m and 1000 m for a velocity of 2.4 - 2.6 is 7.4%, 6.72%, 6.18%, 8.22%, 8.01%. The percentage increase of pressure drop at the depths 600 m, 700 m, 800 m, 900 m and 1000 m for a velocity of 2.6 - 2.8 is 7.66%, 6.67%, 8.66%, 7.23%, 7.2%. The percentage increase of pressure drop at the depths 600 m, 700 m, 800 m,

900 m and 1000 m for a velocity of 2.8 - 3 is 6.58%, 7.69%, 7.14%, 6.22%, 6.25%.

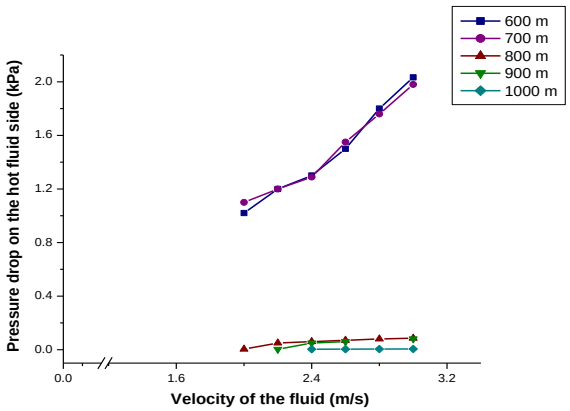

Figure 17. Comparison between the plate length pressure drop on the hot fluid side at various depths

Figure 17 shows the effect of velocity of the fluid on the pressure drop on the hot fluid side for a plate length of 0.7 m at various depths. The pressure drop increases as the velocity of the fluid increases. The percentage increase of pressure drop at the depths 600 m, 700 m, 800 m, 900 m and 1000 m for a velocity of 2-2.2 is 8.32%, 5.76%, 7.59%, 6.3%. The percentage increase of pressure drop at the depths 600 m, 700 m, 800 m, 900 m and 1000m for a velocity of 2.2 - 2.4 is 7.66%, 7.25%,6.18%,8.22%. The percentage increase of pressure drop at the depths 600 m, 700 m, 800 m, 900 m and 1000 m for a velocity of 2.4 - 2.6 is 7.4%, 6.72%, 6.18%, 6.22%. The percentage increase of pressure drop at the depths 600 m, 700 m, 800 m, 900 m and 1000 m for a velocity of 2.6 - 2.8 is 7.66%, 6.77%, 6.96%, 6.66%. The percentage increase of pressure drop at the depths 600 m, 700 m, 800 m, 900 m and 1000 m for a velocity of 2.8 - 3 is 6.58%, 7.69%, 7.14%, 6.22%, 6.25%.

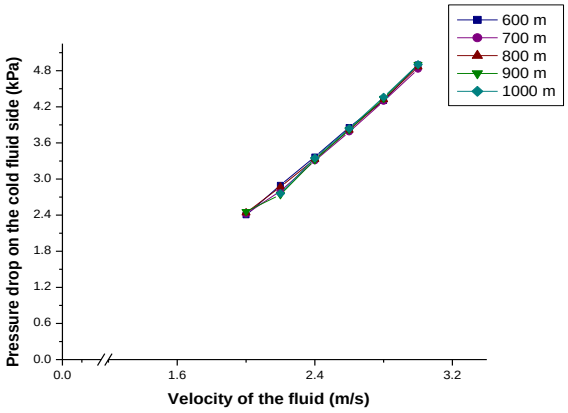

Figure 18. Comparison between the plate length pressure drop on the cold fluid side at various depths

Figure 18 shows the effect of velocity of the fluid on the pressure drop on the cold fluid side for a plate length of 0.7 m at various depths. The pressure drop increases as the velocity of the fluid increases. The percentage increase of pressure drop at the depths 600 m, 700 m, 800 m, 900 m and 1000 m for a velocity of 2 - 2.2 is 8.32%, 5.76%, 6.59%, 6.3%. The percentage increase of pressure drop at the depths 600 m, 700 m, 800 m, 900 m and 1000 m for a velocity of 2.2 - 2.4 is 7.66%, 7.25%, 6.18%, 7.22%, 7.13%. The percentage increase of pressure drop at the depths 600 m, 700 m, 800 m, 900 m and 1000 m for a velocity of 2.4 - 2.6 is 7.4%, 6.72%, 6.18%, 8.22%, 7.98%. The percentage increase of pressure drop at the depths 600 m, 700 m, 800 m, 900 m and 1000 m for a velocity of 2.6 - 2.8 is 7.66%, 8.67%, 8.66%, 9.66%, 8.66%. The percentage increase of pressure drop at the depths 600 m, 700 m, 800 m, 900 m and 1000 m for a velocity of 2.8 - 3 is 7.58%, 7.69%, 8.14%, 6.22%, 6.78%.

Figure 19 shows the effect of velocity of the fluid on the pressure drop on the hot fluid side for a plate length of 0.8 m at various depths. The pressure drop increases as the velocity of the fluid increases. The percentage increase of pressure drop at the depths 600 m, 700 m, 800 m, 900 m and 1000 m for a velocity of 2 - 2.2 is 8.32%, 5.76%, 7.59%, 7.4%, 6.3%. The percentage increase of pressure drop at the depths 600 m, 700 m, 800 m, 900 m and 1000 m for a velocity of 2.2 - 2.4 is 7.66%, 6.25%, 6.18%, 6.0%, 9.22%. The percentage increase of pressure drop at the depths 600 m, 700 m, 800 m, 900 m and 1000 m for a velocity of 2.4 - 2.6 is 9.4%, 7.72%, 6.18%, 7.12%,

8.22%. The percentage increase of pressure drop at the depths 600 m, 700 m, 800 m, 900 m and 1000 m for a velocity of 2.6 - 2.8 is 7.66%, 8.67%, 9.66%, 7.56%, 7.66%. The percentage increase of pressure drop at the depths 600 m, 700 m, 800 m, 900 m and 1000 m for a velocity of 2.8 - 3 is 6.58%, 7.69%, 7.14%, 6.22%, 6.12% .

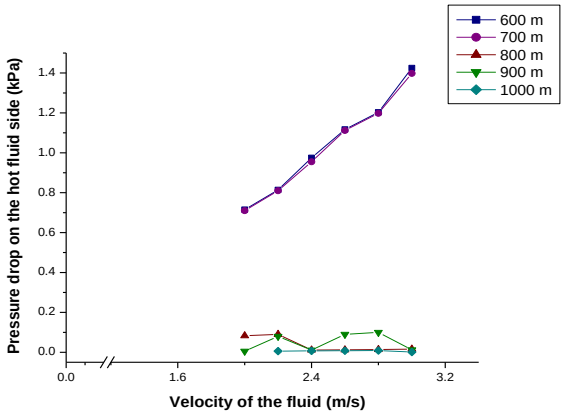

Figure 19. Comparison between the plate length pressure drop on the hot fluid side at various depths

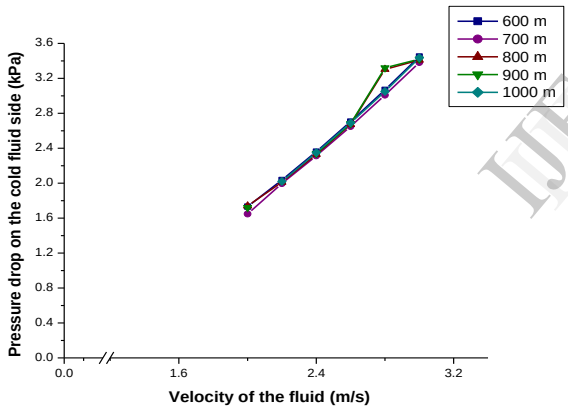

Figure 20. Comparison between the plate length pressure drop on the cold fluid side at various depths

Figure 20 shows the effect of velocity of the fluid on the pressure drop on the hot fluid side for a plate length of 0.8 m at various depths. The pressure drop increases as the velocity of the fluid increases. The percentage increase of pressure drop at the depths 600 m, 700 m, 800 m, 900 m and 1000 m for a velocity of 2 - 2.2 is 8.32%, 6.76%, 8.59%, 7.2%, 7.3%. The percentage increase of pressure drop at the depths 600 m, 700 m, 800 m, 900 m and 1000 m for a velocity of 2.2 - 2.4 is 8.66%, 7.25%, 7.18%, 8.02%, 9.22%. The percentage increase of pressure drop at the depths 600 m, 700 m, 800 m, 900 m and 1000 m for a velocity of 2.4 - 2.6 is 9.4%, 7.72%, 7.18%, 8.26%, 8.22%. The percentage increase of pressure drop at the depths 600 m, 700 m, 800 m, 900 m and 1000 m for a velocity of 2.6 - 2.8 is 8.66%, 8.67%, 9.66%, 8.5%, 8.66%. The percentage increase of pressure drop at the depths 600 m, 700 m, 800 m, 900 m and 1000 m for a velocity of 2.8 - 3 is 8.58%,7.69%, 8.14%, 7.22%, 7.23%, 7.25%.

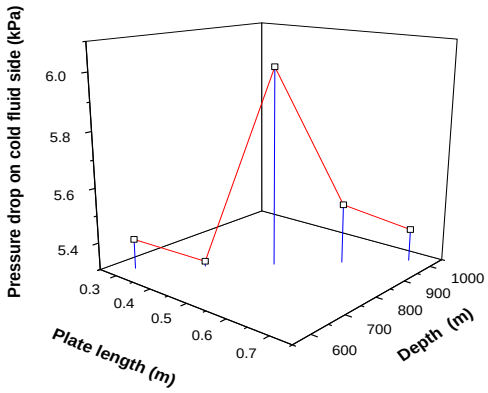

Figure 21. Three dimensional plot of plate length and depth v/s pressure drop on the cold fluid side

Figure 21 shows the 3-D optimized results for the minimum pressure drop on the cold fluid side for various plate lengths and for various depths of the oceans. It is found that the pressure drop is 5.41 for a depth of 600 m at a plate length of 0.3 m. The pressure drop is 5.32 for a depth of 700 m at a plate length of 0.4 m. The pressure drop is 6.012 for a depth of 800 m at a plate length of 0.5 m. The pressure drop is 5.52 for a depth of 900 m at a plate length of 0.6m. The pressure drop is 5.42 for a depth of 1000 m at a plate length of 0.7m. The minimum optimum pressure drop on the cold fluid side is found to be 5.41 at a depth of 700 m.

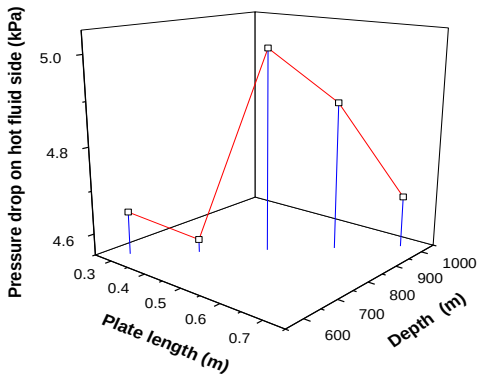

Figure 22. Three dimensional plot of plate length and depth v/s pressure drop on the hot fluid side

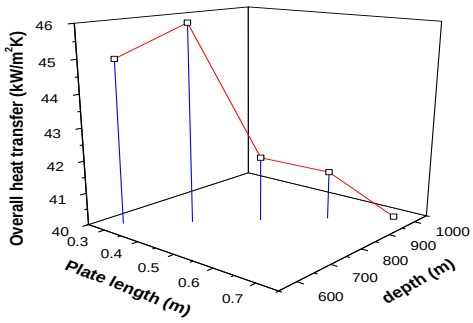

Figure 23. Three dimensional plot of plate length and depth v/s overall heat transfer coefficient

Figure 22 shows the 3-D optimized results for the minimum pressure drop on the hot fluid side for various plate lengths and for various depths of the oceans. It is found that the pressure drop is 4.76 for a depth of 600 m at a plate length of 0.3 m. The pressure drop is 4.58 for a depth of 700 m at a plate length of 0.4 m. The pressure drop is 5.01 for a depth of 800 m at a plate length of 0.5 m. The pressure drop is 4.89 for a depth of 900 m at a plate length of 0.6 m. The pressure drop is 4.67 for a depth of 1000 m at a plate length of 0.7 m. The minimum optimum pressure drop on the cold fluid side is found to be 4.76 at a depth of 700 m.

Figure 23 shows the 3-D optimized results for the Overall heat transfer coefficient on the hot fluid side for various plate lengths and for various depths of the oceans. It is found that the overall heat transfer coefficient increases. The overall heat transfer at a depth of 600 m for a plate length of 0.3 is 45. The overall heat transfer coefficient at a depth of 700 m for a plate length of 0.4 m is 46. The overall heat transfer coefficient at a depth of 800 m for a plate length of 0.5 m is 42. The overall heat transfer coefficient at a depth of 900 m for a plate length of 0.6 m is 41.5. The overall heat transfer coefficient at a depth of 1000 m for a plate length of 0.7 m is 40. The maximum overall heat transfer is found to be 46 at a depth of 700 m

6. Conclusion

In this study, a theoretical approach has been proposed to design a heat exchanger for a 0.1 MWe OTEC plant. Assuming fixed temperature for both hot and cold fluids and varying the pipe length from 0.3 m to 0.7 m and cold fluid suction depth under the ocean from 600 m to 1000 m, a minimum pressure drop and heat transfer co-efficient for both hot and cold fluids is obtained for a certain pipe length and cold fluid suction depth. From the foregoing results, it can be concluded as follows:

1. For varying plate length and depths the pressure drop on the cold fluid side is found to be increasing. The pressure drop on the cold fluid side is found to be feasible for a depth of 700 m with a pressure drop of 5.32 *kPa*.

2. For varying plate length and depths the pressure drop on the hot fluid side is found to be increasing. The pressure drop on the hot fluid side is found to be feasible for a depth of 700 m with a pressure drop of 4.58 *kPa*.

3. For varying plate length and depths the overall heat transfer coefficient is found to be increasing. The overall heat transfer coefficient is found to be feasible for a depth of 700 m with an overall heat transfer coefficient of 46 $kW/m^2 K$.

7. Nomenclature

A	Heat transfer area, m^2
b	Mean spacing between plates, m
C_p	Specific heat capacity, kJ/kgK
D_e	Equivalent diameter, m
D_i	Inner diameter of the tube, m
D_o	Outer diameter of the tube, m
f	Friction factor.
G_m	Mass velocity, kg/m^2s

h	Heat transfer coefficient, W/m^2K
k	Thermal conductivity, W/mK
L	Length of the plate, m
$LMTD$	Log mean temp. difference, $℃$
m	Mass flow rate, kg/s
N	Number of plates
NTU	Number of transfer units.
Nu	Nusselt number
N_p	Number of passes.
Pr	Prandtl number
ΔP	Pressure drop, kPa
Re	Reynolds number
T_{avg}	Average temperature, K
T_c	Temperature of cold fluid, K
T_h	Temperature of hot fluid, K
ΔT	Temperature difference, K
U	Overall heat transfer coefficient kW/m^2K
u	Velocity of the fluid, m/s^2
w	Width of the gasket, m
q	Amount of heat transferred between the fluids, kJ/kgK

Greek Symbols

ρ	Density of the fluid, kg/m^3
μ	Viscosity of the fluid, kg/ms

7. References

[1] H. Blomerius, and N. K. Mitra, "Numerical investigation of convec-tive heat transfer and pressure drop in wavy ducts", Numerical Heat Transfer, 2000, pp. 37–54.

[2] W.W. Focke, and P. G. Knibbe, "Flow visualization in parallel-plate ducts with corrugated walls", J Fluid Mech, Vol. 165, 1986, pp.73–77.

[3] W.W. Focke, J. Zachariades, and L. Olivier, "The effect of the corrugation inclination angle on the thermo hydraulic performance of plate heat exchangers", Int. J Heat Mass Transfer, Vol. 28, 1985, pp. 1469–1497.

[4] R. L. Heavner, H. Kumar, and A.S. Wanniarachchi, "Performance of an industrial plate heat exchanger: effect of chevron angle", Heat Transfer, Am Inst Chem. Eng., AIChE Symp. 295, Vol 89, 1993.

[5] P. J. Heggs, P. Sandham, R. A. Hallam, and C. Walton,"Local transfer coefficients in corrugated plate heat exchangers channels", TransIChemE, Chem.Eng., 1997.

[6] Hesselgraves, J.E., "Compact Heat Exchangers: Selection, Design and Operation", 1st Ed., Pergammon, New York, 2001.

[7] Kays, W.M. and A. L. London, "Compact heat exchangers" 3rdEd. Krieger Publ. Co., Florida, 1998.

[8] K. Mitseuteru, and Y. Ikegami, "The Performance Evaluation of the plate type evaporator using the Ammonia / Water mixtures" Proceeding of the International Conference on Coastal and Ocean Technology, 2003, pp. 365-371.

[9] P. H. G. Allen and T. G. Karayiannis, "Recent Developments in EHD Enhanced Heat Transfer" Renewable Energy, Vol.5, 1995, pp. 436-445.

[10] P. Sriyutha Murthy, R. Venkatesan, K.V.K. Nair, D. Inbakandan, S. Syed Jahan, D. Magesh Peter, and M. Ravindran, "Evaluation of sodium hypochlorite for fouling control in plate heat exchangers for seawater application" International Biodeterioration & Biodegradation, Vol. 55, 2005, 161–170.

[11] S. V. Paras, E. I. P. Drosos, A. J. Karabelas, F. Chopard, "Counter-Current Gas/Liquid Flow Through Channels with Corrugated Walls–Visual Observations of Liquid Distribution and Flooding", World Conference on Experimental Heat Transfer, Fluid Mechanics & Thermodynamics, Thessaloniki, September 24-28, 2001.

[12] S. V. Paras, A.G. Kanaris, A. A. Mouza, A. J. Karabelas, "CFD code application to flow through narrow channels with corrugated walls" International Congress of Chemical and Process Engineering, Prague, 2002.

[13] Shah, R. K. and A. S. Wanniarachi, "Plate heat exchanger design theory", J.M. (Ed.). Industrial Heat Exchangers, Von Karman Institute Lecture Series (1991–2004).

[14] T. Mitsumeri, Y. Ikegami and H. Uehara, "Advantages of plate type heat exchanger over tube type heat exchanger for OTEC power plant", Int. J. Offshore and Polar engg.,Vol .9, 1999.

[15] N. Tsutomo, and H. Uehara, "Shell and tube heat exchangers for OTEC power Plants" Experimental and fluid science, 1988.

[16] H. Uehara, Y. Ikegami, "Optimization of a closed-cycle OTEC system", J. Solar Energy Eng. Vol. 112, 1990, pp. 247–256.

[17] H. Uehara, Y. Ikegami, and K. Tsuboi, "Study on a new OTEC system using ammonia and water as working fluid, JSME Thermal Engineering Conference, 214, 1997, pp. 97-25.

[18] S. Wongwises, "Effect of inclination angles and upper end conditions on the countercurrent flow limitation in straight circular pipes", Int. Comm. Heat Mass Transfer, Vol. 25, 1, 1998, pp. 117-125.

[19] A. Mouza, S. V. Paras, and A. J. Karabelas, "Influence of small tube diameter and inclination angle on flooding phenomena" International Congress of Chemical and Process Engineering, Prague, 2002.